Article

Not peer-reviewed version

Development of a Cost-Effective Process for the Heterologous Production of SARS-CoV-2 Spike Receptor Binding Domain (RBD) Using Pichia pastoris in Stirred-Tank Bioreactor

Diego Noseda , Cecilia D'Alessio , Javier Santos , Tommy Idrovo-Hidalgo , Maria Florencia Pignataro , Diana E Wetzler , Hernán Gentilli , Alejandro D Nadra , Ernesto Roman , Carlos Paván , Lucas AM Ruberto *

Posted Date: 24 April 2023

doi: 10.20944/preprints202304.0821.v1

Keywords: SARS-CoV-2; RBD; ANTIGEN; STBR; PICHIA PASTORIS; BIOREACTOR

Article

Development of a Cost-Effective Process for the Heterologous Production of SARS-CoV-2 Spike Receptor Binding Domain (RBD) Using *Pichia pastoris* in Stirred-Tank Bioreactor

Diego Noseda [1,2], Cecilia D'Alessio [1,3,4], Javier Santos [1,3,4], Tommy Idrovo-Hidalgo [3], Florencia Pignataro F [1,3], Diana E Wetzler [1,4,5], Hernán Gentilli [3], Alejandro D Nadra [1,3], Ernesto Roman [1,4], Carlos Paván [1,7] and Lucas AM Ruberto [6,8,9,*]

[1] Consejo Nacional de Investigaciones Científicas y Técnicas (CONICET), Godoy Cruz 2290, Buenos Aires, Argentina (C1425FQB)
[2] Universidad Nacional de San Martín-CONICET, Instituto de Investigaciones Biotecnológicas (IIBio), Av. 25 de Mayo 1301-1367, Villa Lynch, Provincia de Buenos Aires, Argentina (1650)
[3] Facultad de Ciencias Exactas y Naturales, Departamento de Fisiología y Biología Molecular y Celular, Instituto de Biociencias, Biotecnología y Biología Traslacional (iB3), Ciudad Universitaria- Pabellón II. Buenos Aires, Argentina (1428)
[4] Departamento de Química Biológica, Facultad de Ciencias Exactas y Naturales, Universidad de Buenos Aires, Ciudad Universitaria- Pabellón II. Buenos Aires, Argentina (1428)
[5] CONICET-Universidad de Buenos Aires, Instituto de Química Biológica de la Facultad de Ciencias Exactas y Naturales (IQUIBICEN), Ciudad Universitaria- Pabellón II. Buenos Aires, Argentina (1428)
[6] Departamento de Microbiología, Inmunología, Biotecnología y Genética, Facultad de Farmacia y Bioquímica, Universidad de Buenos Aires, Junín 956 6to piso, Ciudad Autónoma de Buenos Aires, Argentina. (C1113AAD)
[7] Instituto de Química y Fisicoquímica Biológicas, LANAIS PROEM, Facultad de Farmacia y Bioquímica, Universidad de Buenos Aires, Ciudad Autónoma de Buenos Aires, Argentina. (C1113AAD)
[8] CONICET-Universidad de Buenos Aires, Facultad de Farmacia y Bioquímica, Instituto de Nanobiotecnología (NANOBIOTEC), Ciudad Autónoma de Buenos Aires, Argentina. (C1113AAD)
[9] Instituto Antártico Argentino, Ministerio de Relaciones Exteriores y Culto, Buenos Aires, Argentina. Av. 25 de Mayo 1147, Villa Lynch, Provincia de Buenos Aires, Argentina (1650)
* Correspondence: E-mail address: luruberto@gmail.com (Ruberto L); Postal address: Instituto de Nanobiotecnología, Junín 956 6th floor, Ciudad Autónoma de Buenos Aires, Argentina. ZIP Code: C1113AAD

Abstract: SARS-CoV-2 was identified as the pathogenic agent causing the COVID-19 pandemic. Among the proteins codified by this virus, the Spike is one of the most external and exposed. A fragment of the Spike protein, named the Receptor Binding Protein (RBD) interacts with the ACE2 receptors of human cells, allowing the entrance of the viruses. RBD has been proposed as an interesting protein for the development of diagnosis tools, treatment and prevention of the disease. In this work, a method for recombinant RBD production using *Pichia pastoris* as a cell factory in a Stirred Tank Bioreactor (SRTB) up to 7 L was developed. Using a basal saline medium with glycerol, methanol and compressed air in a four stages procedure, around 500 mg/L of raw yRBD (RBD produced by yeasts) and 206 mg/L of purified (>95%) RBD were obtained. Thereby, the proposed method represents a feasible, simple, scalable and cheap procedure for the obtention of RBD for diagnosis kits and vaccines formulation.

Keywords: SARS-CoV-2; RBD; antigen; STBR; *Pichia pastoris*; biorreactor

1. Introduction

The 2020 SARS-CoV-2 pandemic demanded the development of suitable tools to face and manage a widespread human infection. Although massive contagion seems to be nowadays as picture of the recent past, novel viral variants and global increases in the number of infected people,

such as those taking place in China and the North hemisphere during the second semester of 2022, are issues of current concern related to SARS-CoV-2 [1]. Viral proteins or some of its domains would be useful molecules to detect, treat, and prevent viral disease and its consequences. SARS-CoV-2 belongs to the Coronaviridae family [2,3]. Coronaviruses are enveloped non-segmented positive-sense RNA viruses. SARS-CoV-2 virus presents a genome with four open reading frames (ORFs) for the structural proteins: Spike, Envelope, Membrane, and Nucleocapsid. Spike complex (~150 kDa) mediates the viral and cellular membrane interaction and fusion by binding mainly to the angiotensin-converting enzyme 2 (ACE2) through the receptor binding domain (RBD) ([4–7]. Some regions of the Spike protein were suggested as suitable targets for drug development [8]. Considering this specific function, it is possible to assume that RBD heterologous expression would provide a useful tool for diagnosis purposes, as well as for immunization to obtain neutralizing antibodies or even a protein-based vaccine. It was reported that in human natural infection, a large fraction of the neutralizing antibodies target RBD [9–11]. What is more, Liu et al (2020) working with nineteen potent neutralizing antibodies (*in vitro*) obtained from infected patients, found out that almost half of them were directed against the RBD [11], highlighting its potential role as vaccine antigen. For these reasons, SARS-CoV-2 RBD was selected for its heterologous expression aiming to obtain large amounts of such protein.

The heterologous production of several SARS-CoV-2 proteins were reported using different expression systems, being the whole Spike protein and it´s RBD the most common ones [12–15]. For example, Li et al (2020) [16], expressed RBD, the S1 subunit, the WT S ectodomain, and a prefusion trimer-stabilized form of S using Sf9 insect cells.

It is important to consider that Spike protein presents 22 possible N-glycosylations and 4 O-glycosylation sites, being some of them on the RBD domain [17,18]. Additionally, RBD presents 9 cysteines, having 8 of them forming S-S bridges [8]. Glycosylation as well as disulfide bridges are issues of special attention for heterologous protein production, since these kinds of modifications affect protein folding and, in some cases, biological activity [19] . This is particularly relevant when the recombinant proteins are produced for medical use in humans [20,21]. The selection of the expression system is usually strongly conditioned by the requirement of such posttranslational modifications [22]. In the case of RBD, glycosylations and S-S bridges formation seem to be important for adequate protein folding, and thus, expression host selection is a critical decision in the development of its production process [23].

Some yeast such as *Saccharomyces cerevisiae*, *Kluyveromyces lactis*, *Yarrowia lipolytica* and *Pichia pastoris* (*Komagataella phaffii*) are suitable and convenient host for recombinant protein production [24]. Singularly, *P. pastoris* is a methylotrophic non-conventional yeast considered a biological model [25,26] used for heterologous protein production, usually taking advantage of the strong alcohol oxidase 1 (AOX1) promoter and its ability to achieve high cellular density in bioreactors, for which values near 100 g DWC/L were reported [27–29]. The AOX1 promoter strongly responds to methanol while its activity is repressed by glucose and glycerol [30,31]. This yeast is also able to secrete large amounts of properly folded heterologous proteins with only a few other secreted proteins and is, for these reasons, widely used as an expression system. Additionally, this microorganism is able to perform some post translational protein modifications (glycosylation, proteolytic processing and disulfide bonds formation) usually observed in higher eukaryotes, a relevant feature when the production of proteins for medical purposes is involved [32–35], or when the thosel modifications is required for proper protein folding [36–38]. Beyond heterologous protein production, *P. pastoris* has been recently used for the expression of other metabolic pathways leading to the obtention of non-proteinous molecules [39]. It has also been evaluated as a key component in a probiotic preparation for poultry [40]. Finally, a complete reference genome of these microorganisms is available [41].

Optimum conditions for heterologous protein production using *P. pastoris* depend on several factors, such as medium composition, temperature, and culture strategy, among others [42,43]. For this reason, research must be done to find the conditions that maximize protein production with the selected microbial construction [44]. Methanol feeding strategies, flows and concentration are considered as relevant factors affecting cellular activity and protein production [44,45]. Staggered

fed, exponential fed, DO-stat and methanol concentration feedback control are strategies commonly reported for *P. pastoris* cultivation [46]. Among them, DO-Stat consists in looping the methanol feeding to the dissolved oxygen concentration. In such way, methanol feeding is activated as pulses when the % of dissolved oxygen rises beyond a setpoint, thus avoiding an excessive O_2 demand, heat production as well as anaerobiosis or methanol accumulation [47–49].

Antigens such as recombinant RBD are considered useful for subunit vaccines development, especially when they are produced using high yield hosts as *P. pastoris*, allowing the production of large amounts of antigen doses at a relatively low cost [13,14,50], being for this reason and its scalability, suitable tools to face a pandemic.

SARS-CoV-2 pandemic presented nucleic acid-based vaccines as state of the art tools for massive vaccination, however, some safety and logistical aspects of this recently implemented vaccination strategy for humans raised concerns of a great part of the population. Toxicity of synthetic raw materials used to conjugate lipids in mRNA vaccines, the possibility of nucleic acids persisting in vivo and risk of theoretical integration of foreign DNA into the host chromosome [51] in addition to the high costs and strict cold chain requirements for some vaccines based on mRNA -that difficult distribution in remote areas where ultra-low temperature freezers are unavailable-, represent some of its disadvantages. Although this new technology is promising, protein subunit vaccines are also a functional and safe alternative. Due to their higher safety profile, subunit vaccines are primarily developed for use with elderly and infant patients [52,53] and vaccines based on the RBD alone, effectively boost an immune response originally generated against a full-length spike protein trimer, increasing interest in using RBD-based vaccine boosters to provide immunity against emerging variants [54]. Additionally, protein subunit vaccines do not require ultra-freezing conditions and can also be safely stored in a regular fridge or liophilized for their distribution [55], making this type of vaccine, useful for complementing vaccination campaigns all over the world.

In a previous work we reported that recombinant SARS-CoV-2 RBD produced using *P. pastoris* as expression host presents a similar and comparable conformation than the one produced using HEK293T mammalian cells. A bioreactor production procedure was used, yielding 45 mg/L of 90% pure protein [14]. This was a first attempt for the production of RBD at a scale large enough for small-scale protein characterization and immunization assays.

In this work, we propose a new procedure that improves five times the production yield of recombinant RBD antigen from SARS-CoV-2 spike protein. It consists of a 4-step procedure that was optimized by comparing two culture strategies in a 7-L stirred tank bioreactor. Furthermore, we report the scaling up of the procedure of RBD production to a 14-L stirred tank bioreactor.

Goal: The goal of the project is to produce a low-cost antigen to be used in diagnosis (antibodies detection), therapies (generation of neutralizing antibodies), and prevention (vaccine antigen production).

2. Methods

2.1. Plasmid and strain

The RBD sequence and plasmid construction, as well as the *Pichia pastoris* strain used in this work were the same described previously [13,14]. Briefly, the sequence for amino acid residues 319-537 of the SARS-CoV2 spike protein (RBD domain) was codon optimized for expression in *P. pastoris*. Furthermore, the alpha-factor secretion signal (N-terminal) of *S. cerevisiae* was fused to direct the heterologous protein into the culture medium. In addition, a *Staphylococcus aureus* sortase A recognition sequence for covalent coupling and a His6 tag for purification were inserted into the C-terminal extreme. The entire sequence was synthesized and cloned into the pPICZalphaA vector under transcriptional control of the *P. pastoris* AOX1 promoter by GenScript (NJ, USA),. linearized and transformed into *P. pastoris* X-33 strain.

2.2. Determination of dry cell weight

The optical density of *P. pastoris* samples from shake flask cultures and bioreactor fermentations were determined at 600 nm using a UV-Vis spectrophotometer and converted to dry cell weight (DCW, in g/L) using the following equation: DCW=0.269 OD_{600nm} (R^2 = 0.99), corresponding to a calculated DCW to OD_{600nm} calibration curve.

2.3. Quantification of total proteins and RBD

Samples collected during the methanol induction phase of the flask cultures and bioreactor fermentations were centrifuged at 10,000×g for 20 min to obtain cell-free supernatants. Total protein concentration during cultures and fermentations was determined in the supernatants by the Bradford method [56,57] using a calibration curve of the BSA standard. Proteins in the supernatants were run in a 12% SDS-PAGE stained with Coomassie brilliant blue G-250 (Sigma-Aldrich; St. Louis, MO) to visualize protein bands. The relative abundance of recombinant RBD, in both supernatants and purification fractions, were determined by band densitometry using ImageJ software (http://rsb.info.nih.gov/ij) and considering the total protein concentration determined by the Bradford method.

2.4. Medium composition for flask cultures and bioreactor fermentations

Cultivation of *P. pastoris* inoculums in Erlenmeyer flasks were grown either in BMGY medium (1% yeast extract, 2% bactopeptone, 1.34% YNB, 400 µg/L biotin, 100 mM potassium phosphate pH 6 and 1% glycerol) or in low-salt medium (LSM) with 10 g/L glycerol at 28°C and 250 rpm. The LSM medium contains: 4.55 g/L potassium sulfate, 3.73 g/L magnesium sulfate heptahydrate, 1.03 g/L potassium hydroxide, 0.23 g/L calcium sulfate anhydrous, and 10.9 mL/L phosphoric acid 85%. . After sterilization of the medium, 3.5 mL/L of filtered biotin solution (0.2 g/L) and 3.5 mL/L of filtered trace metal solution (PTM1) were added. PTM1 contained per liter: 6.0 g copper (II) sulfate pentahydrate, 0.08 g sodium iodide, 3.0 g manganese sulfate-monohydrate, 0.2 g sodium molybdate-dihydrate, 0.02 g boric acid, 0.5 g cobalt chloride, 20.0 g zinc chloride, 65.0 g ferrous sulfate-heptahydrate, 0.2 g biotin, and 5.0 mL sulfuric acid. Cultivations of *P. pastoris* in bioreactors were performed in LSM supplemented with 40 g/L glycerol. The use of LSM prevents salt precipitation during the pH rise in the downstream process, as was previously reported [58].

2.5. Inoculum preparation

To obtain the inoculum for flask cultures and bioreactor fermentations, a single colony of *P. pastoris* clone grown on a YPD agar plate was inoculated into a 250 mL flask containing 40 mL of LSM (supplemented with PTM1 and biotin) with 10 g/L glycerol or in 250 ml BMGY and cultured overnight at 30 ± 1°C and 250 rpm in an orbital shaker. A volume of 400 mL LSM (supplemented with PTM1 and biotin) containing 10 g/L glycerol in a 2-L Erlenmeyer flask was inoculated with the overnight culture and incubated under the same conditions until the culture reached an OD_{600} of ~ 14. This culture was used to simultaneously inoculate a set of Erlenmeyer flasks and a stirred tank bioreactor with LSM at a ratio of $V_{seed}=V_0/10$, where V_{seed} is the volume of inoculum and V_0 is the initial volume of culture.

2.6. Cultivation in Erlenmeyer flask

Cultures of *P. pastoris* expressing RBD clone were started in Erlenmeyer flasks to evaluate growth kinetics and recombinant RBD production. For this purpose, three 250 mL Erlenmeyer flasks containing 50 mL of LSM (supplemented with PTM1 and biotin) with 10 g/L glycerol were inoculated with 5 mL of the previously described culture and incubated at 30 ± 1°C and 250 rpm in an orbital shaker. After 24 h, induction conditions were established by adding pure methanol at a final concentration of 1% (v/v). This procedure was repeated every 24 hs to maintain methanol induction for a period of 120 hs. During induction, flasks were incubated on shaker at 250 rpm and 25 ± 1°C, as low culture temperatures increase the yield of soluble recombinant proteins in *P. pastoris* due to

reduced extracellular proteolysis without affecting cell growth [59,60]. Culture samples for determination of biomass, total proteins, and RBD concentration were collected every 24 hs. Specific growth rates (μ) for each culture stage were calculated from the slope of the regression line of the growth curve.

2.7. Fermentations in stirred-tank bioreactor

Fermentations were carried out in a stirred-tank bioreactor (BioFlo 115, New Brunswick Scientific; Edison, NJ) using a four-stage procedure based on previous work with modifications [14,61–63]. The first stage consisted of a batch culture using LSM with unlimited glycerol (40 g/L) as the sole carbon and energy source, supplemented with 3.5 mL/L PTM1 and 3.5 mL/L biotin solution (0.2 g/L). After an abrupt peak in the percentage of dissolved oxygen (spike) indicating carbon source depletion, the second phase - fed-batch with glycerol - was initiated. In this phase, the culture was fed with a solution containing 600 g/L of glycerol, 12.25 mL/L PTM1 and 12.25 mL/L biotin solution (0.2 g/L). To ensure glycerol limitation and thus gradually derepress the AOX1 promoter, feeding was automatically regulated according to the percentage of dissolved oxygen (%DO) in the culture, a strategy referred to as DO-stat [47,64]. Later, a short transition phase was performed to allow the adaptation of the culture to growth in the presence of methanol as the sole carbon source. For this, two strategies were compared: 1) feeding with a glycerol/methanol mixture (3:1) for 5 h and 2) feeding with a pulse of 4 g/L of methanol. Finally, the last induction phase was initiated by adding pure methanol, supplemented with 12.25 mL/L PTM1 and 12.25 mL/L biotin solution (0.2 g/L), as the sole carbon and energy source, applying a fed-batch procedure with a growth-limiting rate. The feeding of methanol at limiting concentration was also regulated with the level of DO in the culture (DO-stat). The stirred-tank bioreactor operated in interface with Biocommand Bioprocessing (New Brunswick Scientific) software for parameter control and data acquisition. Temperature was maintained at 30 ± 1°C during the batch and glycerol fed-batch phases and at 25 ± 1°C during the transition and induction phases. The pH was kept at 5.0 in the first two phases and 5.3 in the last two phases by adding 42.5% (v/v) H_3PO_4 and 14% (v/v) NH_4OH, which also served as a nitrogen source. Dissolved oxygen was controlled by stirring (maximum 1000 rpm) and by filtered (0.22 μm) compressed air (1-1.5 VVM). The pH was measured using a pH electrode (Mettler-Toledo GmbH, Germany), and the dissolved oxygen content was determined using a polarographic probe (InPro6110/320, Mettler-Toledo GmbH). Foam formation was prevented by adding 3% (v/v) antifoam agent 204 (Sigma-Aldrich; St. Louis, MO). Samples were taken during the different fermentation phases to determine the concentrations of biomass, total protein, and recombinant RBD. Biomass evolution during fermentation was expressed as DCW (g/L) = f(t). Fermentations were performed in vessels of 7 and 14 liters to compare the RBD production process with two different vessel volumes. After fermentation, biomass was removed from the culture by centrifugation at 18,600 ×g for 20 min at 4°C in a Sorvall high-speed centrifuge (Lynx 4000 Thermo) equipped with a F10 rotor, and the supernatant was used for RBD purification.

2.8. Purification of recombinant RBD and quality control

The purification of recombinant RBD from cell-free supernatants as well as RBD quality control was as already described [14]. Briefly, purification was performed using a NTA-Ni2+ column, previously equilibrated with 20 mM Tris–HCl, 150 mM NaCl, 20 mM imidazol pH 7.4 (equilibration solution). Supernatants were adjusted to pH 7.4 with NaOH, and to 20 mM Tris and 20 mM imidazol, centrifuged 20 min at 12,000×g and loaded into the column. The column was washed with an equilibration solution. Finally, recombinant RBD was eluted in Tris 20 mM, NaCl 150 mM 300 mM imidazole, pH 7.4. The purified protein was dialyzed twice in 20 mM Tris–HCl, 150 mM NaCl buffer, pH 7.4, quantified by UV spectrometry, and stored at −80°C. The purity of recombinant RBD was analyzed by HPLC using a C-18 column.

 doi:10.20944/preprints202304.0821.v1

3. Results

3.1. Growth kinetics and RBD expression at flask level

P. pastoris clone expressing RBD [14] was cultured in Erlenmeyer flasks to evaluate growth kinetics and recombinant RBD expression. The culture in LSM containing 10 g/L glycerol exhibited a maximum specific growth rate (μ_{max}) of 0.15 h^{-1} and a biomass yield coefficient based on consumed substrate ($Y_{X/S}$) of 0.43 g DCW/g glycerol (Figure 1A). At the end of the exponential phase, corresponding to an incubation period of 24 h, the culture displayed a cell concentration of 4.6 g DCW/L while the glycerol was completely depleted. Moreover, during the expression induction phase, in which methanol was added in pulses, cells of the *P. pastoris* clone continued growing with a specific growth rate (μ) of 0.072 h^{-1} in the first 24 h of induction. The culture continued growing, showing a decrease in growth rate, due to methanol limitation, to a final value of 0.002 h^{-1}. Hence, the average specific growth rate over the induction phase was 0.026 h^{-1}. After 120 h of methanol induction, the culture reached a maximum biomass level of 8.0 g DCW/L in the induction phase with a biomass yield coefficient ($Y_{X/S}$) of 0.085 g DCW/g methanol on average (Figure 1A). Figure 1B shows the decrease in specific growth rate during the methanol induction phase.

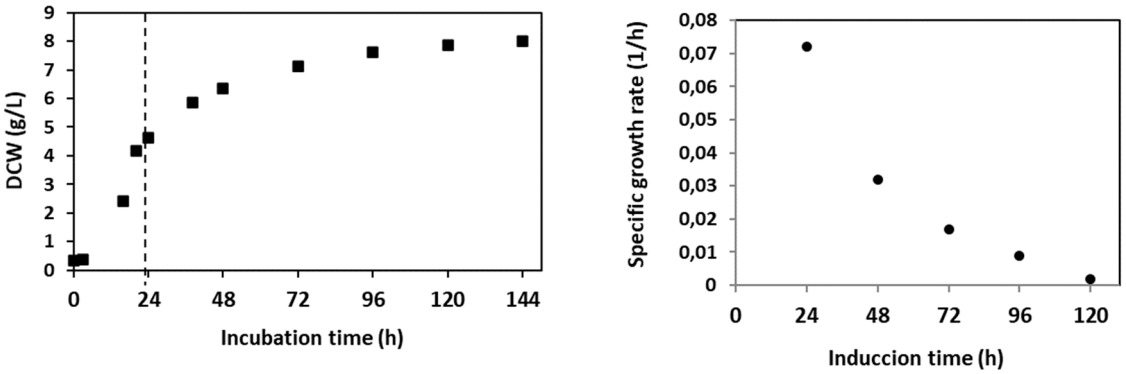

Figure 1. Growth of *P. pastoris* expressing RBD in flask cultures. **A.** Biomass concentration (g DCW/L) evolution during flask cultivation. **P1**: exponential growth phase in LSM glycerol 10 g/L, **P2**: Induction phase with methanol pulses at a final concentration of 1% (v/v), each 24 h incubation. Error bars indicate 2SD. **B.** Variation of the specific growth rate (μ) during the induction phase. During the induction of expression, the culture continued growing with a decrease in growth rate due to the limitation of methanol.

As shown in Table 1, the total protein concentration in the culture supernatant increased from 5.2 mg/L at the beginning of the methanol induction phase to 72.3 mg/L after 120 h of induction. Moreover, the RBD concentration was 1.6 mg/L at the beginning of this phase and 21.7 mg/L at the end, representing a 14-fold increase. The percentage of recombinant RBD in the supernatants with respect to the concentration of total proteins was 30%. The RBD yield based on biomass formation ($Y_{RBD/X}$) showed a value of 2.71 mg/g at 120 h methanol induction, corresponding to an 8-fold increase with respect to the initial value. Furthermore, the volumetric RBD productivity (vP) at the end of incubation was 0.15 mg/Lh, representing an increase of 100% compared to the initial induction time (Table 1). The specific RBD productivity (sP) was 18.8 µg RBD/g DCW h at the end, indicating that this parameter increased 1,4-fold with respect to the initial point (Table 1). Finally, the RBD yield based on methanol consumed ($Y_{RBD/S}$) reached 0.54 mg RBD/g methanol at the end of the whole process. It is worth mentioning that the results obtained with Erlenmeyer cultures are important for planning the scale-up of recombinant RBD production in the stirred tank bioreactor.

Preprints (www.preprints.org) | NOT PEER-REVIEWED | Posted: 24 April 2023 doi:10.20944/preprints202304.0821.v1

Table 1. Parameters obtained from the culture of P. pastoris expressing RBD in Erlenmeyer flasks. YP/X (mgRBD / g DCW): RBD yield based on biomass formation; vP (mg RBD/L h): volumetric RBD productivity, sP (ug RBD/g DCW h): specific RBD productivity.

Induction time (h)	Total protein (mg/L)	RBD (mg/L)	RBD increase (fold)	Yp/x (mg/g)	vP (mg/L h)	sP (ug/g h)
0	5.2	1.6	1.0	0.34	0.07	14.1
24	12.8	3.8	2.5	0.61	0.08	12.7
48	26.4	7.9	5.1	1.12	0.11	15.5
72	41.8	12.5	8.0	1.67	0.13	17.4
96	57.1	17.1	11.0	2.17	0.14	18.1
120	72.3	21.7	13.9	2.71	0.15	18.8

3.2. Production of recombinant RBD in 7-L stirred bioreactor

Fermentation of the *P. pastoris* clone for the production of recombinant RBD was first performed in a 7-L stirred tank bioreactor according to the four-phase procedure described above. Two fermentation strategies were compared, using an initial culture volume of 1.5 liters in the bioreactor in both cases. The fermentation carried out with strategy 1 showed a maximum biomass concentration of 16.7 g DCW/L at 18 h of the batch phase. During this stage, the *P. pastoris* culture displayed a maximum specific growth rate (μ_{max}) of 0.16 h^{-1} and a biomass yield coefficient ($Y_{X/S}$) of 0.42 DCW/g glycerol. After an increase in dissolved oxygen due to glycerol depletion (DO spike), the fed-batch phase was initiated, with glycerol feeding controlled by the percentage of dissolved oxygen (%DO), with a cut-off of 50 % saturation. Glycerol feeding was maintained for 23 h reaching a biomass level of 61.4 g DCW/L. Next, the transition phase was performed by feeding the culture with a glycerol:methanol (3:1) mixture for 5 h, allowing the cells to adapt to the methanol and reaching a cell concentration of 64.1 g DCW/L at the end of this phase. Then, the methanol-fed batch phase was carried out to induce the expression of recombinant RBD, regulating the feeding of pure methanol in response to %DO with a saturation cut-off of 60%. After 52 h of methanol induction and a total fermentation process of 98 h, the culture reached a biomass level of 78.2 g DCW/L. At this fermentation time, the total protein concentration in the culture supernatant was 296.3 mg/L, while RBD reached 98.4 mg/L, corresponding to 33% of the total proteins in the supernatant (Table 2). Since the volume of the supernatant was 2.6 L, a total amount of RBD of 255.8 mg was obtained. The RBD yield based on biomass formation ($Y_{RBD/X}$) exhibited a value of 1.3 mg RBD/g DCW at the end of the induction. The volumetric RBD productivity (vP) of the whole process reached 1.0 mg RBD/L h and the total RBD productivity ($_{T}P$) was 2.6 mg RBD/h (Table 2). Moreover, the specific RBD productivity of the whole process was 12.8 µg RBD/g DCW h and the RBD yield based on methanol consumed ($Y_{RBD/S}$) reached 0.5 mg DCW/g methanol at the end of the fermentation.

Preprints (www.preprints.org) | NOT PEER-REVIEWED | Posted: 24 April 2023 doi:10.20944/preprints202304.0821.v1

Table 2. Production parameters of *Pichia pastoris* fermentations using strategies 1 and 2 in 7 L stirred tank bioreactor. Detailed production parameters: Final biomass level (g DCW/L), Total protein concentration (mg/L); RBD concentration (mg/L); Total RBD (mg); $Y_{RBD/biomass}$ (RBD yield based on biomass formation, mg/g); whole process volumetric RBD productivity (vP, mg RBD/L h), whole process specific RBD productivity (sP, ug RBD/g DCW h), $Y_{RBD/Methanol}$: (RBD yield based on methanol consumed, mg/g).

	Strategy 1	Strategy 2
Final biomass level (g DCW/L)	78.2	89.2
Total Protein level (mg/L)	296.3	1378.5
RBD concentration (mg/L)	98.4	519.6
Total RBD (mg)	255.8	1402.9
Y_{RBD}/biomass (mg/g)	1.3	5.8
RBD volumetric productivity (mg/L h)	1.0	3.8
RBD total productivity (mg/h)	2.6	10.3
RBD specific productivity (ug/g DCW h)	12.8	42.2
Y_{RBD}/methanol (mg/g)	0.5	1.8

The fermentation performed with strategy 2 in the 7-L stirred bioreactor presented a maximum biomass level of 17.2 g DCW/L at the end of batch phase (18 h). At this stage, the culture showed similar values of specific growth rate and biomass yield coefficient as in strategy 1. In the fed-batch phase, feeding with glycerol was maintained for 8 h in response to %DO with a saturation cut-off of 50%, reaching a biomass level of 40.9 g DCW/L. Then, in the transition phase, feeding was carried out with a dose of 4 g/L methanol, which allowed culture adaptation to methanol and to reach a biomass concentration of 41.4 g DCW/L after 4 h. Complete consumption of methanol was indicated by an abrupt increase of %DO (DO spike). During the induction phase, methanol feeding was regulated by %DO with a saturation cut-off of 60%, reaching a final biomass level of 89.2 g DCW/L after 108 h of induction and 138 h of total process. At this time, the total protein and RBD concentrations in the culture reached 1378.5 mg/L and 519.6 mg/L, respectively, while the total recombinant RBD yielded 1402.9 mg, as the supernatant volume was 2.7 L (Table 2). Thereby, the RBD yield based on biomass ($Y_{RBD/X}$) at the end of the process showed a value of 5.8 mg RBD/g DCW, an increase of 4.5-fold compared to strategy 1. The volumetric RBD productivity (vP) of the whole process was 3.8 mg RBD/L h and the total RBD productivity ($_{T}P$) reached 10.3 mg RBD/h (Table 2), which corresponds to an approximately 4-fold increase of both parameters compared to strategy 1. Moreover, the specific RBD productivity of the whole process was 42.2 µg RBD/g DCW h and the RBD yield based on methanol consumed ($Y_{RBD/S}$) reached 1.8 mg RBD/g methanol at the end of the fermentation, corresponding to an approximately 3.5-fold increase of both parameters compared to strategy 1. Figure 2 shows the parameter profile of the fermentation carried out with strategy 2 and describes the variation of stirring, temperature, pH, dissolved oxygen and feeding throughout the fermentation process. This profile reports the decrease in dissolved oxygen content due to culture growth during the batch phase until the dissolved oxygen spike, the point at which glycerol feeding began, and also shows the variations in dissolved oxygen content by which glycerol or methanol feeding was regulated. SDS-PAGE analysis of fermentation supernatants corresponding to strategy 2 displayed the increase in total protein and recombinant RBD during the expression induction phase with methanol. The bands corresponding to the different glycosylated variants of the RBD antigen have molecular weights of 40, 35 and 30 kDa (Figure 3A). In addition, Figure 3B describes the increase in total proteins and RBD concentration, as well as the percentage of RBD in total proteins every 12 h of

Preprints (www.preprints.org) | NOT PEER-REVIEWED | Posted: 24 April 2023 doi:10.20944/preprints202304.0821.v1

the methanol induction phase corresponding to the fermentation performed with strategy 2. Table 3 describes the evolution of the production parameters during the fermentation carried out with strategy 2 in the 7 L stirred bioreactor. It should be noted that the RBD concentration increased more than 20-fold during the induction and the percentage of RBD in total proteins increased from 26.5% to 37.7% at the end of the induction phase.

Table 3. Evolution of production parameters during fermentation carried out with strategy 2 in 7 L stirred tank bioreactor: Detailed parameters every 12 h of methanol induction: Total protein concentration (mg/L); RBD concentration (mg/L); RBD percentage respect total protein (%): RBD concentration increase (fold); $Y_{P/X}$: RBD yield based on biomass formation (mg/g); vP: volumetric RBD productivity (mg RBD/L h).

Induction time (h)	Total protein concentration (mg/L)	RBD concentration (mg/L)	RBD percentage (%)	RBD increase (fold)	$Y_{P/X}$ (mg/g)	vP (mg/L h)
0	85.0	22.6	26.5	1.0	0.5	0.8
12	168.7	48.2	28.6	2.1	0.8	1.2
24	207,7	66.0	31.8	2.9	1.0	1.2
36	241.0	81.7	33.9	3.6	1.1	1.3
48	328.5	112.3	34.2	5.0	1.4	1.5
60	435.0	149.6	34.4	6.6	1.9	1.7
72	570.6	198.6	34.8	8.8	2.4	2.0
84	711.4	256.8	36.1	11.4	2.9	2.3
96	1178.3	439.8	37.3	19.5	4.9	3.5
108	1378.5	519.6	37.7	23.0	5.8	3.8

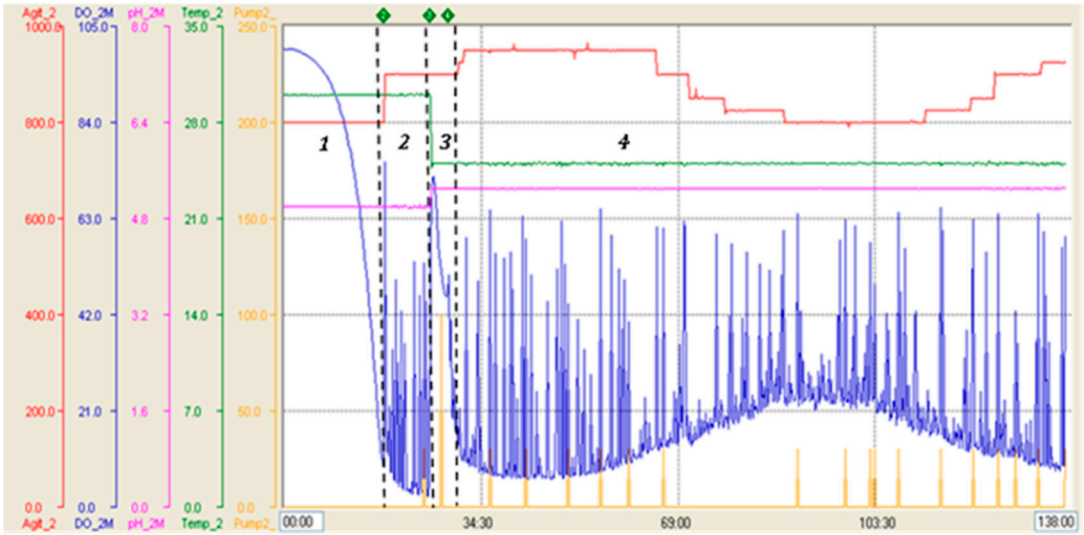

Figure 2. Parameters profile of fermentations carried out with strategy 2 in 7 L stirred tank bioreactor. Blue line: dissolved oxygen level (saturation percentage), green line: temperature (°C), pink line: pH, red line: stirring (RPM), yellow line: feeding (pumping percentage)**.** 1: Batch phase, 2: Glycerol fed-batch phase, 3: Transition phase, 4: Induction phase.

Preprints (www.preprints.org) | NOT PEER-REVIEWED | Posted: 24 April 2023 doi:10.20944/preprints202304.0821.v1

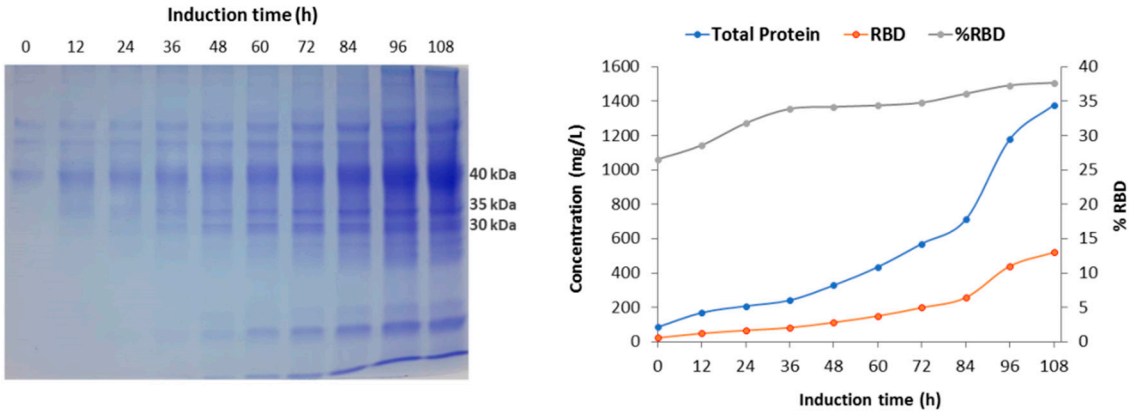

Figure 3. SDS-PAGE analysis and production parameters of samples from the induction phase of 7-L bioreactor fermentation. **A:** SDS-PAGE protein profile of fermentation supernatants corresponding to methanol induction phase. Molecular weights indicate the different glycosylated RBD variants. **B:** Variation in total proteins concentration, RBD concentration and RBD percentage in total protein during methanol induction.

3.3. Scale-up of recombinant RBD production in a 14-L stirred tank bioreactor

After fermentation in a 7-L bioreactor, RBD production was scaled up in a 14-L stirred tank bioreactor with an initial volume of 4 liters and using strategy 2 as a four-step procedure. In the batch phase, a biomass concentration of 17.6 g DCW/L was achieved after 18 h, reaching similar μ_{max} and $Y_{X/S}$ values to those previously obtained. Next, in the fed-batch phase, glycerol feeding was performed for 8 h, in response to %DO with a saturation cut-off of 60%, obtaining a biomass concentration of 41.7 g DCW/L. The transition phase was started by supplying the culture with a dose of 4 g/L methanol as the sole carbon and energy source. A biomass level of 42.5 g DCW/L was achieved after 4 h. During the subsequent fed-batch induction phase, feeding of pure methanol was done using a DO-Stat strategy, in which methanol feeding was controlled in response to %DO with a saturation cut-off of 60%. After 115 h of methanol induction and a total fermentation process of 145 h, the fermented culture reached a final biomass level of 90.3 g DCW/L. At this time, the total protein concentration in the fermented culture was 1032.7 mg/L, while the RBD concentration reached 533.4 mg/L, corresponding to 51.7% of the total proteins in the supernatant.

The total recombinant RBD was 2987 mg, as the volume of the supernatant was 5.6 L (Table 4). The RBD yield based on biomass ($Y_{RBD/X}$) at the end of fermentation was 5.9 mg RBD/g DCW, the volumetric RBD productivity (vP) of the whole process reached 3.7 mg RBD/L h, and the total RBD productivity ($_{T}P$) was 20.7 mg RBD/h (Table 4). Moreover, the specific RBD productivity (sP) of the whole process reached 40.7 µg RBD/g DCW h and the RBD yield based on methanol consumed ($Y_{RBD/S}$) was 1.9 mg RBD/g methanol at the end of the induction period. It is important to note that the values obtained for RBD yield based on biomass ($Y_{RBD/X}$), volumetric productivity (vP) and specific productivity (sP) of the whole process were similar to those obtained with the 7 L bioreactor applying strategy 2, indicating that the scale-up was successful.

Preprints (www.preprints.org) | NOT PEER-REVIEWED | Posted: 24 April 2023 doi:10.20944/preprints202304.0821.v1

Table 4. Evolution of production parameters during fermentation carried out with strategy 2 in 14 L stirred-tank bioreactor: Detailed parameters every 24 h of methanol induction: Total protein concentration (mg/L); RBD concentration (mg/L); RBD percentage respect total protein (%); RBD concentration increase (fold); $Y_{P/X}$: RBD yield based on biomass formation (mg/g); vP: whole process volumetric RBD productivity (mg RBD/L h).

Induction time (h)	Total protein concentration (mg/L)	RBD concentration (mg/L)	RBD percentage (%)	RBD increase (fold)	Yp/x (mg/g)	Pv (mg/L h)
0	120.3	37.3	31.0	1.0	1.0	1.2
24	169.7	65.2	38.4	1.7	1.1	1.2
48	237.0	101.2	42.7	2.7	1.4	1.3
72	415.3	188.1	45.3	5.0	2.4	1.8
96	669.2	321.8	48.1	8.6	3.9	2.6
115	1032.7	533.4	51.7	14.3	5.9	3.7

The parameters profile of the fermentation shown on Figure 4 specifically displays the variation of stirring, dissolved oxygen and feeding during the process. It shows the decrease of DO level in the batch phase until its abrupt increase (DO spike) and later the variations of dissolved oxygen that controlled the feeding of glycerol and methanol. The SDS -PAGE analysis reveals the increase in total protein and recombinant RBD during the induction phase with methanol (Figure 5A). It is worth mentioning that the glycosylated variants of the recombinant RBD correspond to the diffuse bands of around 40, 35, and 30 kDa. Figure 5B shows the increase in total proteins and RBD concentration, as well as the percentage of RBD in total proteins every 24 h of the induction phase. The RBD concentration increased more than 14-fold and the percentage of RBD in total proteins increased from 31 % to 52% at the end of such a phase.

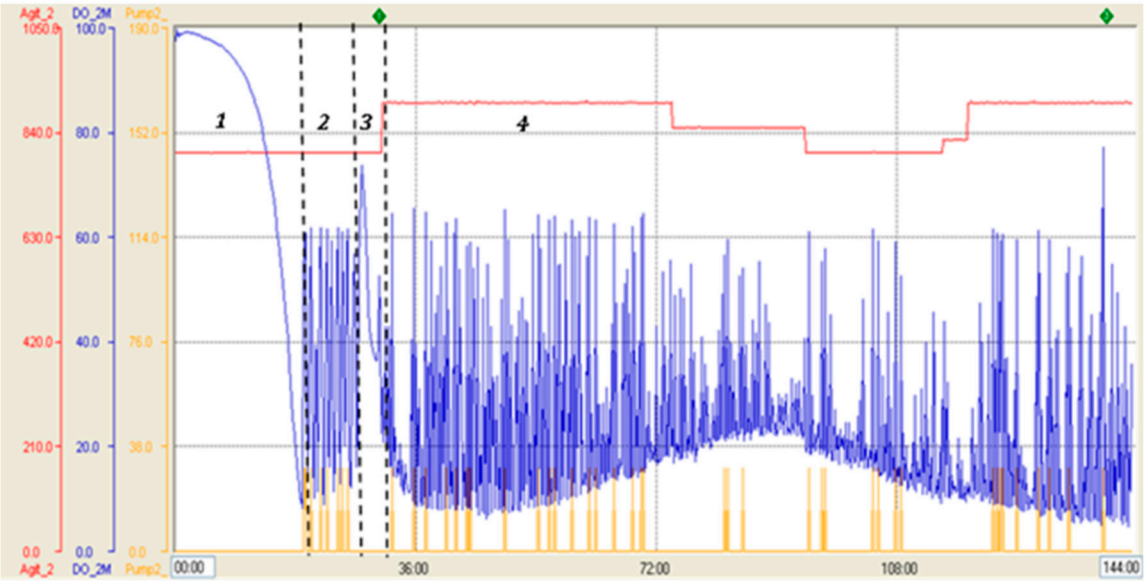

Preprints (www.preprints.org) | NOT PEER-REVIEWED | Posted: 24 April 2023 doi:10.20944/preprints202304.0821.v1

Figure 4. Parameter profile of fermentation carried out in 14 L stirred tank bioreactor with strategy 2. Blue line: dissolved oxygen level (saturation percentage), red line: stirring (RPM), yellow line: feeding (pumping percentage). 1: Batch phase, 2: Glycerol fed-batch phase, 3: Transition phase, 4: Induction phase.

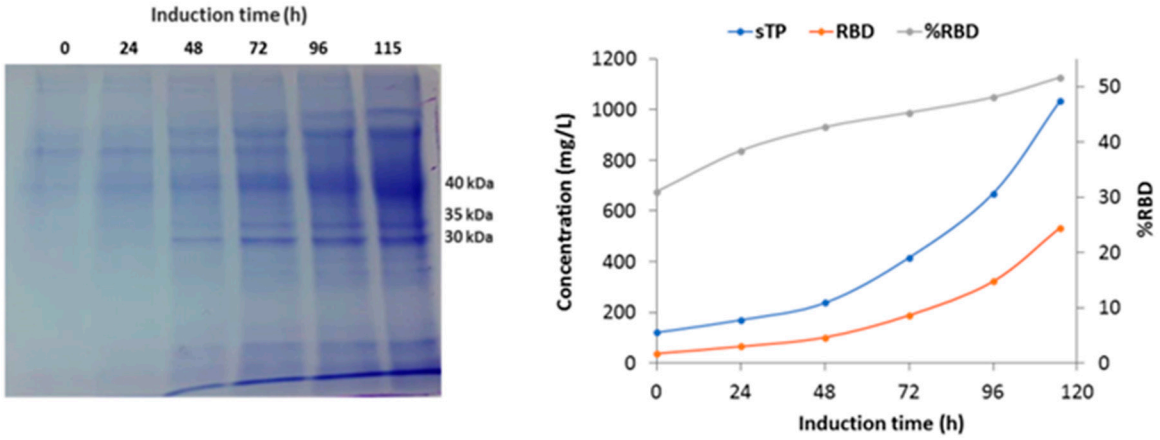

Figure 5. SDS-PAGE analysis and production parameters of the induction phase in a 14-L bioreactor fermentation performed with strategy 2. A: SDS-PAGE total protein profile of fermentation supernatants corresponding to induction phase. Molecular weights indicate the different glycosylated RBD variants. B: Variation in total proteins concentration, RBD concentration and RBD percentage in total protein during methanol induction.

3.4. Purification and analysis of RBD

RBD was recovered from the fermentation supernatant as already described [14]. Briefly, 1-2 liter fractions of supernatant were purified in a single step using 20 mL of a Ni2+-NTA affinity column. Pure RBD was eluted using imidazol as a competitor, and the protein was dialyzed with Tris 20 mM, NaCl 150 mM, pH 7.4. Protein was obtained at more than 95% purity as evaluated by HPLC analysis (Figure 6).

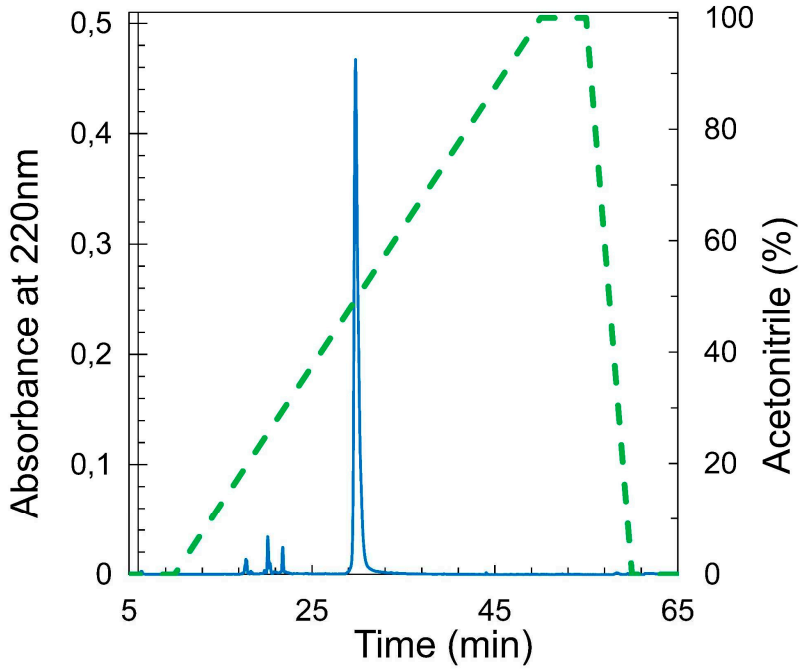

 doi:10.20944/preprints202304.0821.v1

Figure 6. Analysis by RP-HPLC of RBD produced in *P. pastoris* and purified by NTA-Ni²⁺. Analytical C18 reverse-phase HPLC chromatogram for RBD produced in *P. pastoris* (20 ug) was obtained upon an ACN gradient 0 to 100% over 40 min (10- 50 min of the run, dashed line) and with a mobile phase of 0.05% TFA. The integration of the main peak was 95 % (filled line).

4. Discussion

As a quick response to the SARS-CoV-2 pandemic, several research groups around the world started to develop biological tools to provide raw materials for diagnosis, treatment and prevention of the disease. In such a context, during 2020, we reported the production of SARS-CoV-2 RBD domain using *P. pastoris* as a cell factory. We also compared its structural features with RBD produced in mammalian HEK293T cells to verify that they were similar [14]. As the next step, in this article we describe a rational procedure for SARS-CoV2 RBD production scaling up in *P. pastoris* up to 7 L. To do that, two different culture strategies were tested, showing strategy 2, a combination of batch and fed-batch using a DO-stat feeding, the best performance by allowing the obtention of more than 500 mg/L of raw yRBD in the culture broth. This cultivation procedure represents a simple, robust, scalable and low-cost method since it involves the use of a stirred tank bioreactor (STBR), a defined basal salt medium with simple carbon sources (glycerol and methanol) and the provision of oxygen exclusively from compressed air, avoiding the use of pure O_2 and its associated risks [65,66]. This affirmation is especially valid when comparing RBD production with other expression hosts such as eukaryotic cells [67,68]. Additionally, the use of a defined saline medium, avoiding or minimizing the requirement of complex undefined ingredients, allows the monitoring of component concentrations throughout the cultivation period, which is considered as a valuable feature for industrial processes [69]. All these advantages turn RDB produced in *P. pastoris* following the procedure reported here into an attractive molecule to be used in diagnostic tools or for vaccine developments, especially considering its cost and easiness.

Based on the specific growth rate (μ) obtained during the first 24 h of induction (0.072 h^{-1}) of Erlenmeyer flask cultivation, it can be surmised that this recombinant clone behaves as a Mut^+ strain, as expected. In this sense, Orman *et al*. [70] reported a maximum specific growth rate (μ_{max}) of 0.16 h^{-1} for a recombinant *P. pastoris* clone expressing hGH in a defined medium with methanol as the sole carbon and energy source . Pla *et al*. [71], working with Mut^+ and Mut^s clones expressing scFV obtained a μ_{max} of 0.044 h^{-1} and 0.015 h^{-1} respectively. A recent study proposes that the use of Mut^+ phenotype is convenient for high levels of heterologous protein production considering that pAOX1 is induced not only by methanol but also by its metabolites formaldehyde and formate [72]. So, a high methanol utilization results in a stronger pAOX1 induction increasing heterologous protein production compared to a lower methanol utilization metabolism. These authors reported that the Mut^+ clone showed a specific β-galactosidase (heterologous protein) expression rate 5 and 10-fold higher than the Mut^s and Mut^- ones. In our work, the observed Mut^+ phenotype could be one of the reasons supporting the high level of RBD expression.

It is well established that an adequate induction phase design is crucial for high heterologous protein titers in *P. pastoris* when the AOX1 promoter is used [73,74]. In our procedure the transition phase from glycerol was done as a pure methanol pulse to achieve a concentration of 4 g/L in the culture broth followed by the induction phase under a DO-stat feeding for 108 h. The criteria underlying this design are related to providing enough methanol for adaptation and induction minimizing the risk of methanol accumulation as well as keeping O_2 demand and heat production controlled. Some methanol feeding strategies keeping its concentration constant or within a defined range has been reported for heterologous protein production in *P. pastoris* and *P. methanolica* [75,76]. These strategies allow a strong and constant AOX1 induction while avoiding methanol accumulation and the consequent cell intoxication. Several analytical methods to achieve this feeding profile have been developed [77,78]. Most of them require specific and expensive equipment. Considering such arguments, the strategy applied in this work emerges as an alternative procedure when permanent methanol concentration surveillance is not available. The induction strategy used in this work is based and shares some features with those reported by Yamawaki *et al* [45] for the production of an

 doi:10.20944/preprints202304.0821.v1

antibody fragment (scFv). For induction, these authors combined a stage in which methanol concentration was kept at 15.7 g/L for 5 hs (controlled by a methanol sensor feedback) followed by a DO-stat for 36 hs (total induction time: 41 hs). Under these conditions, 247 mg/L of recombinant protein was obtained. In the case of the process reported here, cells in the bioreactor were exposed to a significant but non-toxic methanol level (4 g/L) adequate for AOX1 activation. Adaptation stage end was deducted from a O_2 spike, indicator of methanol exhaustion and a signal to start methanol fed-batch under a DO-stat strategy. So, we combined an adaptation stage with a methanol pulse and the subsequent induction of the RBD expression with methanol feeding in response to %DO in the culture broth as a production strategy.

Using this procedure, around 500 mg/L of RBD were obtained solubilized in the culture broth. Further purification steps resulted in the obtention of 206.4 mg/L of pure protein (95%). This amount of recombinant protein was significantly higher than those obtained and reported previously (96.1 mg/L of total RBD and 45 mg/L of 95% pure protein) representing approximately a ~ 5-fold improvement [14].

Other authors [79,80] reported the production of 400 mg/L of a recombinant SARS-CoV2 RBD219-N1 using *P. pastoris* X-33. For this purpose, these authors developed a multistage process including several fed flows and gradients. In that case, the induction stage took ~70 h. During the process, %DO was maintained above 30% adjusting gas provision and agitation. These authors did not report the gas provision source (air or O_2).

In a recent article [81], the production of a modified SARS-CoV-2 RBD using *P. pastoris* X-33 at a 50 L scale was reported. The production process is based on a saline medium containing yeast extract and other elements (histidine, biotin, myo-innositol, calcium pantothenate, pyridoxal hydrochloride, thiamine di-hydrochloride and nicotinic acid). The process involved the use of constant feedings rates and yielded a dry cell weight of 58.15 g/L, and 68.38 mg/L of RBD. Downstream consisted in an IMAC (Cu^{2+}) followed by a semi-preparative RP-HPLC. After that, recombinant RBD showed a purity equal to or higher than 98%. The bioreactor culture lasted for 38 to 48 h. Both DCW and RBD concentration were lower than those obtained under the proposed procedure (90 g/L vs 58 g/L and 500 mg/L vs 68 mg/L). However, fermentation time is shorter in the procedure reported by [81], providing a potential advantage for industrial production.

Methanol metabolism by alcohol oxidase is a process that requires high levels of oxygen and releases a large amount of energy as heat. *P. pastoris* high density cultures using this substrate are usually carried out providing pure oxygen. The DO-stat strategy applied for both glycerol fed-batch and methanol induction resulted in a moderate O_2 consumption and a gradual heat production.

As was stated by [82] costs associated with heterologous protein production using microorganisms are driven by medium composition and cooling. The cultivation method proposed in this work is coherent with this affirmation, considering that it involves the use of a simple and relatively cheap medium and a DO stat strategy, thus diminished oxygenation and cooling requirements.

In the case of prokaryotic hosts, RBD is usually obtained as a non-glycosylated, non-folded protein. For this reason, re-folding is needed during downstream processing. Related to that, the production of RBD was reported using *E. coli* as an expression system. [83] developed a production method using a BL21 strain obtaining most RDB in inclusion bodies. After solubilization and renaturalization, they recovered 65.2% of the produced RBD by Nickel affinity chromatography, reporting a production yield of 13.3 mg/L. Meena *et al.* [84] also informed RBD production in bacterial cells as inclusion bodies. These authors cultivated a *E. coli* strain carrying the RBD gene in Erlenmeyer flask containing 1 L of a complex not defined media (a modification of the Luria Bertani broth), ampicillin and IPTG induction. After cultivation, they obtained 62.10 mg of raw RBD as inclusion bodies from 1 L of culture. After that, several downstream steps were needed, including solubilization at pH 12.5 and 3, refolding and DEAE chromatography.

RBD obtained from this process is a glycosylated protein showing three main variants (30, 35 and 40 kDa). These variants present the same primary structure differing only in the glycosylation pattern [14]. Beyond its crucial function in protein folding, glycosylation represents an issue of special

concern for RBD industrial production, since the intra- and inter-batch heterogeneity could be considered as a drawback for standardization and regulations compliance [85]. Further research is needed to clarify the impact of this post-translacional modification on biological activity and to improve protein homogeneity. We are currently working on several factors to improve protein homogeneity.

In summary, in this work we presented an efficient and reliable scaling up method for the production of a low cost RBD antigen using the methylotrophic yeast *P. pastoris*, with multiple advantages. One possible drawback of this procedure is the extension of the induction stage. This extension is partially caused by the DO-stat strategy, which involves a kind of "dead time" among methanol feeding pulses. These periods are minutes in which no, or very low levels of methanol are available in the culture broth, probably resulting in a waste of time for the metabolic machinery of *P. pastoris*. As an alternative, a strategy in which methanol concentration is kept constant, could be more effective. However, this strategy would require a method for real time methanol concentration evaluation, through a GC associated method or a specific detector, which requires specific equipment. As the strategy 2 resulted in the obtention of a well folded, immunologically active RBD we propose the method provided here to scale up the production of RBD.

5. Conclusion

Industrial production of recombinant proteins, especially those for pharmaceutical products, draw upon different living organisms as hosts, harnessing their advantages while dealing with their disadvantages [86,87]. There is no universal host for this task and each protein can be produced "conveniently" in a process meeting a swarm of factors, being protein features (structure and posttranslational modifications), production performance and costs, protein application and legal regulations some of the most relevant. Here we proposed such a convenient process for RBD production.

CRediT authorship contribution statement: Noseda D: Methodology, Investigation, Writing-original draft, Visualization. **D´Alessio C:** Conceptualization, **I**nvestigation, Methodology**,** Resources, Writing-Review & Editing**,** Funding acquisition, Project administration, **Santos J:** Funding acquisition, Writing-Review & Editing, Project administration**, Idrovo-Hidalgo T:** Methodology**,** Investigation**. Pignataro F:** Methodology, Investigation. **Wetzler DE:** Methodology, Resources**. Gentilli H:** Methodology**. Nadra AD:** Funding acquisition**,** Conceptualization**,** Project administration, Writing - Review & Editing. **Roman E:** Methodology and validation. **Paván C:** Methodology. **Ruberto L:** Conceptualization, Investigation, Methodology, Writing original draft, Project administration.

Funding: This work was supported partially by the grants IP COVID - 19 – 234 and PICTO 2021-0007 provided by the ANPCYT (Argentina).

Data availability: Data will be made available on request

Acknowledgements: We'd like to thank the Consorcio Argentino AntiCovid for helpful discussions and collaborative work during the pandemic.

Declaration of Competing Interest: The authors declare that they have no known competing financial interests or personal relationships that could have appeared to influence the work reported in this paper. The strain and some steps of the processes presented are included in the Pending patents PCT/US22/43578 and AR P210102579.

References

1. Dennehy, J.J.; Gupta, R.K.; Hanage, W.P.; Johnson, M.C.; Peacock, T.P. Where Is the next SARS-CoV-2 Variant of Concern? *Lancet* **2022**, *399*, 1938–1939, doi:10.1016/S0140-6736(22)00743-7.
2. Forster, P.; Forster, L.; Renfrew, C.; Forster, M. Phylogenetic Network Analysis of SARS-CoV-2 Genomes. *Proceedings of the National Academy of Sciences* 2020, *117*, 9241–9243.
3. Wang, X.-M.; Mannan, R.; Xiao, L.; Abdulfatah, E.; Qiao, Y.; Farver, C.; Myers, J.L.; Zelenka-Wang, S.; McMurry, L.; Su, F.; et al. Characterization of SARS-CoV-2 and Host Entry Factors Distribution in a COVID-19 Autopsy Series. *Communications Medicine* 2021, *1*.

4. Arimori, T.; Takagi, J. Structure of SARS-CoV-2 Spike Receptor-Binding Domain Complexed with High Affinity ACE2 Mutant 3N39 2020.
5. Xu, Z.P.; Liu, K.F.; Han, P.; Qi, J.X. Structure of SARS-CoV-2 Spike Receptor-Binding Domain Complexed with Its Receptor Equine ACE2 2022.
6. Wang, X.; Lan, J.; Ge, J.; Yu, J.; Shan, S. Crystal Structure of SARS-CoV-2 Spike Receptor-Binding Domain Bound with ACE2 2020.
7. Lan, J.; Ge, J.; Yu, J.; Shan, S.; Zhou, H.; Fan, S.; Zhang, Q.; Shi, X.; Wang, Q.; Zhang, L.; et al. Structure of the SARS-CoV-2 Spike Receptor-Binding Domain Bound to the ACE2 Receptor. *Nature* 2020, *581*, 215–220.
8. Shamsi, A.; Mohammad, T.; Anwar, S.; Amani, S.; Khan, M.S.; Husain, F.M.; Rehman, M.T.; Islam, A.; Hassan, M.I. Potential Drug Targets of SARS-CoV-2: From Genomics to Therapeutics. *International Journal of Biological Macromolecules* 2021, *177*, 1–9.
9. Ju, B.; Zhang, Q.; Ge, J.; Wang, R.; Sun, J.; Ge, X.; Yu, J.; Shan, S.; Zhou, B.; Song, S.; et al. Human Neutralizing Antibodies Elicited by SARS-CoV-2 Infection. *Nature* **2020**, *584*, 115–119, doi:10.1038/s41586-020-2380-z.
10. Greaney, A.J.; Starr, T.N.; Barnes, C.O.; Weisblum, Y.; Schmidt, F.; Caskey, M.; Gaebler, C.; Cho, A.; Agudelo, M.; Finkin, S.; et al. Mapping Mutations to the SARS-CoV-2 RBD That Escape Binding by Different Classes of Antibodies. *Nat. Commun.* **2021**, *12*, 1–14, doi:10.1038/s41467-021-24435-8.
11. Liu, L.; Wang, P.; Nair, M.S.; Yu, J.; Rapp, M.; Wang, Q.; Luo, Y.; Chan, J.F.-W.; Sahi, V.; Figueroa, A.; et al. Potent Neutralizing Antibodies against Multiple Epitopes on SARS-CoV-2 Spike. *Nature* **2020**, *584*, 450–456, doi:10.1038/s41586-020-2571-7.
12. Fujita, R.; Hino, M.; Ebihara, T.; Nagasato, T.; Masuda, A.; Lee, J.M.; Fujii, T.; Mon, H.; Kakino, K.; Nagai, R.; et al. Efficient Production of Recombinant SARS-CoV-2 Spike Protein Using the Baculovirus-Silkworm System. *Biochem. Biophys. Res. Commun.* **2020**, *529*, 257–262, doi:10.1016/j.bbrc.2020.06.020.
13. Argentinian AntiCovid Consortium Covalent Coupling of Spike's Receptor Binding Domain to a Multimeric Carrier Produces a High Immune Response against SARS-CoV-2. *Sci. Rep.* **2022**, *12*, 692, doi:10.1038/s41598-021-03675-0.
14. Argentinian AntiCovid Consortium Structural and Functional Comparison of SARS-CoV-2-Spike Receptor Binding Domain Produced in Pichia Pastoris and Mammalian Cells. *Sci. Rep.* **2020**, *10*, 21779, doi:10.1038/s41598-020-78711-6.
15. Smith, I.; Mc Callum, G.J.; Sabljic, A.V.; Marfía, J.I.; Bombicino, S.S.; Trabucchi, A.; Iacono, R.F.; Birenbaum, J.M.; Vázquez, S.C.; Minoia, J.M.; et al. Rapid and Cost-Effective Process Based on Insect Larvae for Scale-up Production of SARS-COV-2 Spike Protein for Serological COVID-19 Testing. **2021**, doi:10.1002/bit.27889.
16. Li, T.; Zheng, Q.; Yu, H.; Wu, D.; Xue, W.; Xiong, H.; Huang, X.; Nie, M.; Yue, M.; Rong, R.; et al. SARS-CoV-2 Spike Produced in Insect Cells Elicits High Neutralization Titres in Non-Human Primates. *Emerg. Microbes Infect.* **2020**, *9*, 2076–2090, doi:10.1080/22221751.2020.1821583.
17. Shajahan, A.; Supekar, N.T.; Gleinich, A.S.; Azadi, P. Deducing the N- and O-Glycosylation Profile of the Spike Protein of Novel Coronavirus SARS-CoV-2. *Glycobiology* **2020**, *30*, 981–988, doi:10.1093/glycob/cwaa042.
18. Azad, T.; Singaravelu, R.; Taha, Z.; Jamieson, T.R.; Boulton, S.; Crupi, M.J.F.; Martin, N.T.; Brown, E.E.F.; Poutou, J.; Ghahremani, M.; et al. Nanoluciferase Complementation-Based Bioreporter Reveals the Importance of N-Linked Glycosylation of SARS-CoV-2 S for Viral Entry. *Molecular Therapy* 2021, *29*, 1984–2000.
19. Jenkins, N.; Curling, E.M. Glycosylation of Recombinant Proteins: Problems and Prospects. *Enzyme Microb. Technol.* **1994**, *16*, 354–364, doi:10.1016/0141-0229(94)90149-x.
20. Brooks, S.A. Appropriate Glycosylation of Recombinant Proteins for Human Use. *Mol. Biotechnol.* **2004**.
21. Lingg, N.; Zhang, P.; Song, Z.; Bardor, M. The Sweet Tooth of Biopharmaceuticals: Importance of Recombinant Protein Glycosylation Analysis. *Biotechnol. J.* **2012**, *7*, 1462–1472, doi:10.1002/biot.201200078.
22. Goh, J.B.; Ng, S.K. Impact of Host Cell Line Choice on Glycan Profile. *Crit. Rev. Biotechnol.* **2018**.
23. Casalino, L.; Gaieb, Z.; Goldsmith, J.A.; Hjorth, C.K.; Dommer, A.C.; Harbison, A.M.; Fogarty, C.A.; Barros, E.P.; Taylor, B.C.; McLellan, J.S.; et al. Beyond Shielding: The Roles of Glycans in the SARS-CoV-2 Spike Protein. *ACS Cent Sci* **2020**, *6*, 1722–1734, doi:10.1021/acscentsci.0c01056.
24. Vieira Gomes, A.M.; Souza Carmo, T.; Silva Carvalho, L.; Mendonça Bahia, F.; Parachin, N.S. Comparison of Yeasts as Hosts for Recombinant Protein Production. *Microorganisms* **2018**, *6*, doi:10.3390/microorganisms6020038.

25. Bernauer, L.; Radkohl, A.; Lehmayer, L.G.K.; Emmerstorfer-Augustin, A. Komagataella Phaffii as Emerging Model Organism in Fundamental Research. *Front. Microbiol.* **2020**, *11*, 607028, doi:10.3389/fmicb.2020.607028.
26. Ata, Ö.; Ergün, B.G.; Fickers, P.; Heistinger, L.; Mattanovich, D.; Rebnegger, C.; Gasser, B. What Makes Komagataella Phaffii Non-Conventional? *FEMS Yeast Res.* **2021**, *21*, doi:10.1093/femsyr/foab059.
27. Wegner, G.H. Emerging Applications of the Methylotrophic Yeasts. *FEMS Microbiol. Rev.* **1990**, *7*, 279–283, doi:10.1111/j.1574-6968.1990.tb04925.x.
28. Daly, R.; Hearn, M.T.W. Expression of Heterologous Proteins in Pichia Pastoris: A Useful Experimental Tool in Protein Engineering and Production. *J. Mol. Recognit.* **2005**, *18*, 119–138, doi:10.1002/jmr.687.
29. Ergün, B.G.; Berrios, J.; Binay, B.; Fickers, P. Recombinant Protein Production in Pichia Pastoris: From Transcriptionally Redesigned Strains to Bioprocess Optimization and Metabolic Modelling. *FEMS Yeast Res.* **2021**, *21*, doi:10.1093/femsyr/foab057.
30. Hartner, F.S.; Glieder, A. Regulation of Methanol Utilisation Pathway Genes in Yeasts. *Microb. Cell Fact.* **2006**, *5*, 39, doi:10.1186/1475-2859-5-39.
31. Hartner, F.S.; Ruth, C.; Langenegger, D.; Johnson, S.N.; Hyka, P.; Lin-Cereghino, G.P.; Lin-Cereghino, J.; Kovar, K.; Cregg, J.M.; Glieder, A. Promoter Library Designed for Fine-Tuned Gene Expression in Pichia Pastoris. *Nucleic Acids Research* 2008, *36*, e76–e76.
32. Cereghino, G.P.L.; Lin Cereghino, G.P.; Sunga, A.J.; Cereghino, J.L.; Cregg, J.M. Expression of Foreign Genes in the Yeast Pichia Pastoris. *Genetic Engineering: Principles and Methods* 157–169.
33. Cregg, J.M.; Cereghino, J.L.; Shi, J.; Higgins, D.R. Recombinant Protein Expression in Pichia Pastoris. *Molecular Biotechnology* 2000, *16*, 23–52.
34. Cereghino, G.P.L.; Cereghino, J.L.; Ilgen, C.; Cregg, J.M. Production of Recombinant Proteins in Fermenter Cultures of the Yeast Pichia Pastoris. *Curr. Opin. Biotechnol.* **2002**, *13*, 329–332, doi:10.1016/s0958-1669(02)00330-0.
35. Cereghino, J.L.; Cregg, J.M. Heterologous Protein Expression in the Methylotrophic Yeast Pichia Pastoris. *FEMS Microbiol. Rev.* **2000**, *24*, 45–66, doi:10.1111/j.1574-6976.2000.tb00532.x.
36. Shental-Bechor, D.; Levy, Y. Effect of Glycosylation on Protein Folding: A Close Look at Thermodynamic Stabilization. *Proc. Natl. Acad. Sci. U. S. A.* **2008**, *105*, 8256–8261, doi:10.1073/pnas.0801340105.
37. Jayaprakash, N.G.; Surolia, A. Role of Glycosylation in Nucleating Protein Folding and Stability. *Biochem. J* **2017**, *474*, 2333–2347, doi:10.1042/BCJ20170111.
38. Roth, J.; Zuber, C.; Park, S.; Jang, I.; Lee, Y.; Kysela, K.G. Protein N-Glycosylation, Protein Folding, and Protein Quality Control. *Molecules* **2010**.
39. Gao, J.; Jiang, L.; Lian, J. Development of Synthetic Biology Tools to Engineer Pichia Pastoris as a Chassis for the Production of Natural Products. *Synth Syst Biotechnol* **2021**, *6*, 110–119, doi:10.1016/j.synbio.2021.04.005.
40. Gaboardi, G.C.; Alves, D.; Gil de Los Santos, D.; Xavier, E.; Nunes, A.P.; Finger, P.; Griep, E.; Roll, V.; Oliveira, P.; Silva, A.; et al. Influence of Pichia Pastoris X-33 Produced in Industrial Residues on Productive Performance, Egg Quality, Immunity, and Intestinal Morphometry in Quails. *Sci. Rep.* **2019**, *9*, 15372, doi:10.1038/s41598-019-51908-0.
41. Sturmberger, L.; Chappell, T.; Geier, M.; Krainer, F.; Day, K.J.; Vide, U.; Trstenjak, S.; Schiefer, A.; Richardson, T.; Soriaga, L.; et al. Refined Pichia Pastoris Reference Genome Sequence. *J. Biotechnol.* **2016**, *235*, 121–131, doi:10.1016/j.jbiotec.2016.04.023.
42. Sinha, J.; Plantz, B.A.; Zhang, W.; Gouthro, M.; Schlegel, V.; Liu, C.-P.; Meagher, M.M. Improved Production of Recombinant Ovine Interferon-Tau by Mut(+) Strain of Pichia Pastoris Using an Optimized Methanol Feed Profile. *Biotechnol. Prog.* **2003**, *19*, 794–802, doi:10.1021/bp025744q.
43. Files, D.; Ogawa, M.; Scaman, C.H.; Baldwin, S.A. A Pichia Pastoris Fermentation Process for Producing High-Levels of Recombinant Human Cystatin-C. *Enzyme Microb. Technol.* **2001**, *29*, 335–340, doi:10.1016/S0141-0229(01)00395-7.
44. Cos, O.; Ramón, R.; Montesinos, J.L.; Valero, F. Operational Strategies, Monitoring and Control of Heterologous Protein Production in the Methylotrophic Yeast Pichia Pastoris under Different Promoters: A Review. *Microb. Cell Fact.* **2006**, *5*, 17, doi:10.1186/1475-2859-5-17.
45. Yamawaki, S.; Matsumoto, T.; Ohnishi, Y.; Kumada, Y.; Shiomi, N.; Katsuda, T.; Lee, E.K.; Katoh, S. Production of Single-Chain Variable Fragment Antibody (scFv) in Fed-Batch and Continuous Culture of

Pichia Pastoris by Two Different Methanol Feeding Methods. *J. Biosci. Bioeng.* **2007**, *104*, 403–407, doi:10.1263/jbb.104.403.

46. Looser, V.; Bruhlmann, B.; Bumbak, F.; Stenger, C.; Costa, M.; Camattari, A.; Fotiadis, D.; Kovar, K. Cultivation Strategies to Enhance Productivity of Pichia Pastoris: A Review. *Biotechnol. Adv.* **2015**, *33*, 1177–1193, doi:10.1016/j.biotechadv.2015.05.008.
47. Ferreira, A.R.; Ataíde, F.; von Stosch, M.; Dias, J.M.L.; Clemente, J.J.; Cunha, A.E.; Oliveira, R. Application of Adaptive DO-Stat Feeding Control to Pichia Pastoris X33 Cultures Expressing a Single Chain Antibody Fragment (scFv). *Bioprocess Biosyst. Eng.* **2012**, *35*, 1603–1614, doi:10.1007/s00449-012-0751-z.
48. Trinh, L.B.; Phue, J.N.; Shiloach, J. Effect of Methanol Feeding Strategies on Production and Yield of Recombinant Mouse Endostatin from Pichia Pastoris. *BioTechnology* **2003**.
49. Liu, W.; Xiang, H.; Zhang, T.; Pang, X.; Su, J.; Liu, H. Development of a New High-Cell Density Fermentation Strategy for Enhanced Production of a Fungus β-Glucosidase in Pichia Pastoris. *Frontiers in* **2020**.
50. Dalvie, N.C.; Rodriguez-Aponte, S.A. Engineered SARS-CoV-2 Receptor Binding Domain Improves Manufacturability in Yeast and Immunogenicity in Mice. *Proceedings of the* **2021**.
51. Liu, Y.; Ye, Q. Nucleic Acid Vaccines against SARS-CoV-2. *Vaccines (Basel)* **2022**, *10*, doi:10.3390/vaccines10111849.
52. Jain, S.; Venkataraman, A.; Wechsler, M.E.; Peppas, N.A. Messenger RNA-Based Vaccines: Past, Present, and Future Directions in the Context of the COVID-19 Pandemic. *Adv. Drug Deliv. Rev.* **2021**, *179*, 114000, doi:10.1016/j.addr.2021.114000.
53. Heidary, M.; Kaviar, V.H.; Shirani, M.; Ghanavati, R.; Motahar, M.; Sholeh, M.; Ghahramanpour, H.; Khoshnood, S. A Comprehensive Review of the Protein Subunit Vaccines Against COVID-19. *Front. Microbiol.* **2022**, *13*, 927306, doi:10.3389/fmicb.2022.927306.
54. Dalvie, N.C.; Tostanoski, L.H.; Rodriguez-Aponte, S.A.; Kaur, K.; Bajoria, S.; Kumru, O.S.; Martinot, A.J.; Chandrashekar, A.; McMahan, K.; Mercado, N.B.; et al. SARS-CoV-2 Receptor Binding Domain Displayed on HBsAg Virus-like Particles Elicits Protective Immunity in Macaques. *Sci Adv* **2022**, *8*, eabl6015, doi:10.1126/sciadv.abl6015.
55. Ghasemiyeh, P.; Mohammadi-Samani, S.; Firouzabadi, N.; Dehshahri, A.; Vazin, A. A Focused Review on Technologies, Mechanisms, Safety, and Efficacy of Available COVID-19 Vaccines. *Int. Immunopharmacol.* **2021**, *100*, 108162, doi:10.1016/j.intimp.2021.108162.
56. Kruger, N.J. The Bradford Method for Protein Quantitation. *Protein Protocols Handbook, The* 15–22.
57. Kruger, N.J. The Bradford Method for Protein Quantitation. In *Springer Protocols Handbooks*; Humana Press: Totowa, NJ, 2009; pp. 17–24 ISBN 9781603274746.
58. Chen, W.-H.; Chag, S.M.; Poongavanam, M.V.; Biter, A.B.; Ewere, E.A.; Rezende, W.; Seid, C.A.; Hudspeth, E.M.; Pollet, J.; McAtee, C.P.; et al. Optimization of the Production Process and Characterization of the Yeast-Expressed SARS-CoV Recombinant Receptor-Binding Domain (RBD219-N1), a SARS Vaccine Candidate. *J. Pharm. Sci.* **2017**, *106*, 1961–1970, doi:10.1016/j.xphs.2017.04.037.
59. Li, Z.; Xiong, F.; Lin, Q.; d'Anjou, M.; Daugulis, A.J.; Yang, D.S.; Hew, C.L. Low-Temperature Increases the Yield of Biologically Active Herring Antifreeze Protein in Pichia Pastoris. *Protein Expr. Purif.* **2001**, *21*, 438–445, doi:10.1006/prep.2001.1395.
60. Shi, X.; Karkut, T.; Chamankhah, M.; Alting-Mees, M.; Hemmingsen, S.M.; Hegedus, D. Optimal Conditions for the Expression of a Single-Chain Antibody (scFv) Gene in Pichia Pastoris. *Protein Expr. Purif.* **2003**, *28*, 321–330, doi:10.1016/s1046-5928(02)00706-4.
61. Celik, E.; Calık, P. Production of Recombinant Proteins by Yeast Cells. *Biotechnol. Adv.* **2012**, *30*, 1108–1118, doi:10.1016/j.biotechadv.2011.09.011.
62. Noseda, D.G.; Recúpero, M.N.; Blasco, M.; Ortiz, G.E.; Galvagno, M.A. Cloning, Expression and Optimized Production in a Bioreactor of Bovine Chymosin B in Pichia (Komagataella) Pastoris under AOX1 Promoter. *Protein Expr. Purif.* **2013**, *92*, 235–244, doi:10.1016/j.pep.2013.08.018.
63. Noseda, D.G.; Recúpero, M.; Blasco, M.; Bozzo, J.; Galvagno, M.Á. Production in Stirred-Tank Bioreactor of Recombinant Bovine Chymosin B by a High-Level Expression Transformant Clone of Pichia Pastoris. *Protein Expr. Purif.* **2016**, *123*, 112–121, doi:10.1016/j.pep.2016.03.008.
64. Picotto, L.D.; Sguazza, G.H.; Tizzano, M.A.; Galosi, C.M.; Cavalitto, S.F.; Pecoraro, M.R. An Effective and Simplified DO-Stat Control Strategy for Production of Rabies Glycoprotein in Pichia Pastoris. *Protein Expr. Purif.* **2017**, *132*, 124–130, doi:10.1016/j.pep.2017.02.004.

65. Westwood, M.-M.; Rieley, W. Medical Gases, Their Storage and Delivery. *Anaesthesia & Intensive Care Medicine* **2012**, *13*, 533–538, doi:10.1016/j.mpaic.2012.09.004.
66. Malayaman, S.N.; Mychaskiw, G., II; Berry, J.M.; Ehrenwerth, J. Medical Gases: Storage and Supply. In *Anesthesia Equipment*; Elsevier, 2021; pp. 3–24.
67. Farnós, O.; Venereo-Sánchez, A.; Xu, X.; Chan, C.; Dash, S.; Chaabane, H.; Sauvageau, J.; Brahimi, F.; Saragovi, U.; Leclerc, D.; et al. Rapid High-Yield Production of Functional SARS-CoV-2 Receptor Binding Domain by Viral and Non-Viral Transient Expression for Pre-Clinical Evaluation. *Vaccines (Basel)* **2020**, *8*, doi:10.3390/vaccines8040654.
68. Li, W.; Fan, Z.; Lin, Y.; Wang, T.-Y. Serum-Free Medium for Recombinant Protein Expression in Chinese Hamster Ovary Cells. *Front. Bioeng. Biotechnol.* **2021**, *9*, 646363, doi:10.3389/fbioe.2021.646363.
69. Zhang, J.; Greasham, R. Chemically Defined Media for Commercial Fermentations. *Appl. Microbiol. Biotechnol.* **1999**.
70. Orman, M.A.; Çalık, P.; Özdamar, T.H. The Influence of Carbon Sources on Recombinant-human-growth-hormone Production by Pichia Pastoris Is Dependent on Phenotype: A Comparison of Muts and Mut+ …. *Biotechnol. Appl. Biochem.* **2009**.
71. Pla, I.A.; Damasceno, L.M.; Vannelli, T.; Ritter, G.; Batt, C.A.; Shuler, M.L. Evaluation of Mut+ and MutS Pichia Pastoris Phenotypes for High Level Extracellular scFv Expression under Feedback Control of the Methanol Concentration. *Biotechnol. Prog.* **2006**, *22*, 881–888, doi:10.1021/bp060012+.
72. Singh, A.; Narang, A. The Mut+ Strain of Komagataella Phaffii (Pichia Pastoris) Expresses PAOX1 5 and 10 Times Faster than Muts and Mut− Strains: Evidence That Formaldehyde Or/and Formate Are True Inducers of PAOX1. *Appl. Microbiol. Biotechnol.* **2020**, *104*, 7801–7814, doi:10.1007/s00253-020-10793-8.
73. Barrigón, J.M.; Montesinos, J.L.; Valero, F. Searching the Best Operational Strategies for Rhizopus Oryzae Lipase Production in Pichia Pastoris Mut+ Phenotype: Methanol Limited or Methanol Non-Limited …. *Biochem. Eng. J.* **2013**.
74. Garrigós-Martínez, J.; Nieto-Taype, M.A. Specific Growth Rate Governs AOX1 Gene Expression, Affecting the Production Kinetics of Pichia Pastoris (Komagataella Phaffii) PAOX1-Driven Recombinant …. *Microb. Cell Fact.* **2019**.
75. Mayson, B.E.; Kilburn, D.G.; Zamost, B.L.; Raymond, C.K.; Lesnicki, G.J. Effects of Methanol Concentration on Expression Levels of Recombinant Protein in Fed-Batch Cultures of Pichia Methanolica. *Biotechnol. Bioeng.* **2003**, *81*, 291–298, doi:10.1002/bit.10464.
76. Katakura, Y.; Zhang, W.; Zhuang, G.; Omasa, T. Effect of Methanol Concentration on the Production of Human β2-Glycoprotein I Domain V by a Recombinant Pichia Pastoris: A Simple System for the Control of Methanol …. *J. Ferment. Bioeng.* **1998**.
77. Guarna, M.M.; Lesnicki, G.J.; Tam, B.M.; Robinson, J.; Radziminski, C.Z.; Hasenwinkle, D.; Boraston, A.; Jervis, E.; MacGillivray, R.T.; Turner, R.F.; et al. On-Line Monitoring and Control of Methanol Concentration in Shake-Flask Cultures of Pichia Pastoris. *Biotechnol. Bioeng.* **1997**, *56*, 279–286, doi:10.1002/(SICI)1097-0290(19971105)56:3<279::AID-BIT5>3.0.CO;2-G.
78. Schenk, J.; Marison, I.W.; von Stockar, U. A Simple Method to Monitor and Control Methanol Feeding of Pichia Pastoris Fermentations Using Mid-IR Spectroscopy. *J. Biotechnol.* **2007**, *128*, 344–353, doi:10.1016/j.jbiotec.2006.09.015.
79. Chen, W.-H.; Du, L.; Chag, S.M.; Ma, C.; Tricoche, N.; Tao, X.; Seid, C.A.; Hudspeth, E.M.; Lustigman, S.; Tseng, C.-T.K.; et al. Yeast-Expressed Recombinant Protein of the Receptor-Binding Domain in SARS-CoV Spike Protein with Deglycosylated Forms as a SARS Vaccine Candidate. *Hum. Vaccin. Immunother.* **2014**, *10*, 648–658, doi:10.4161/hv.27464.
80. Chen, W.H.; Hotez, P.J.; Bottazzi, M.E. Potential for Developing a SARS-CoV Receptor-Binding Domain (RBD) Recombinant Protein as a Heterologous Human Vaccine against Coronavirus Infectious Disease …. *Hum. Vaccin.* **2020**.
81. An Engineered SARS-CoV-2 Receptor-Binding Domain Produced in Pichia Pastoris as a Candidate Vaccine Antigen. *N. Biotechnol.* **2022**, *72*, 11–21, doi:10.1016/j.nbt.2022.08.002.
82. Cardoso, V.M.; Campani, G.; Santos, M.P.; Silva, G.G. Cost Analysis Based on Bioreactor Cultivation Conditions: Production of a Soluble Recombinant Protein Using Escherichia Coli BL21 (DE3). *Biotechnology* **2020**.

83. He, Y.; Qi, J.; Xiao, L.; Shen, L.; Yu, W.; Hu, T. Purification and Characterization of the Receptor-Binding Domain of SARS-CoV-2 Spike Protein from Escherichia Coli. *Eng. Life Sci.* **2021**, *21*, 453–460, doi:10.1002/elsc.202000106.
84. Meena, J.; Singhvi, P.; Srichandan, S.; Dandotiya, J.; Verma, J.; Singh, M.; Ahuja, R.; Panwar, N.; Wani, T.Q.; Khatri, R.; et al. RBD Decorated PLA Nanoparticle Admixture with Aluminum Hydroxide Elicit Robust and Long Lasting Immune Response against SARS-CoV-2. *Eur. J. Pharm. Biopharm.* **2022**, *176*, 43–53, doi:10.1016/j.ejpb.2022.05.008.
85. Hossler, P.; Khattak, S.F.; Li, Z.J. Optimal and Consistent Protein Glycosylation in Mammalian Cell Culture. *Glycobiology* **2009**, *19*, 936–949, doi:10.1093/glycob/cwp079.
86. Dumont, J.; Euwart, D.; Mei, B.; Estes, S.; Kshirsagar, R. Human Cell Lines for Biopharmaceutical Manufacturing: History, Status, and Future Perspectives. *Crit. Rev. Biotechnol.* **2016**, *36*, 1110–1122, doi:10.3109/07388551.2015.1084266.
87. Kiss, B.; Gottschalk, U.; Pohlscheidt, M. *New Bioprocessing Strategies: Development and Manufacturing of Recombinant Antibodies and Proteins*; Springer, 2018; ISBN 9783319971100.